

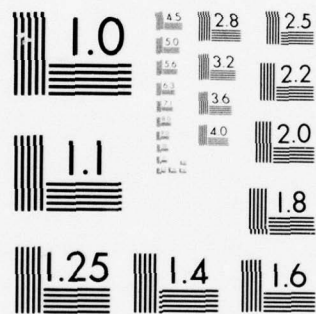
AD-A040 299

BEDFORD INST OF OCEANOGRAPHY DARTMOUTH (NOVA SCOTIA) --ETC F/G 4/2
A COMPARISON OF THE AIR-SEA INTERACTION FLUX MEASUREMENT SYSTEM--ETC(U)
DEC 76 S D SMITH, R J ANDERSON, E G BANKE N00014-76-C-0446
BI-R-76-17 NL

UNCLASSIFIED

| OF |
AD
A040299





MICROCOPY RESOLUTION TEST CHART
NATIONAL BUREAU OF STANDARDS-1963-A

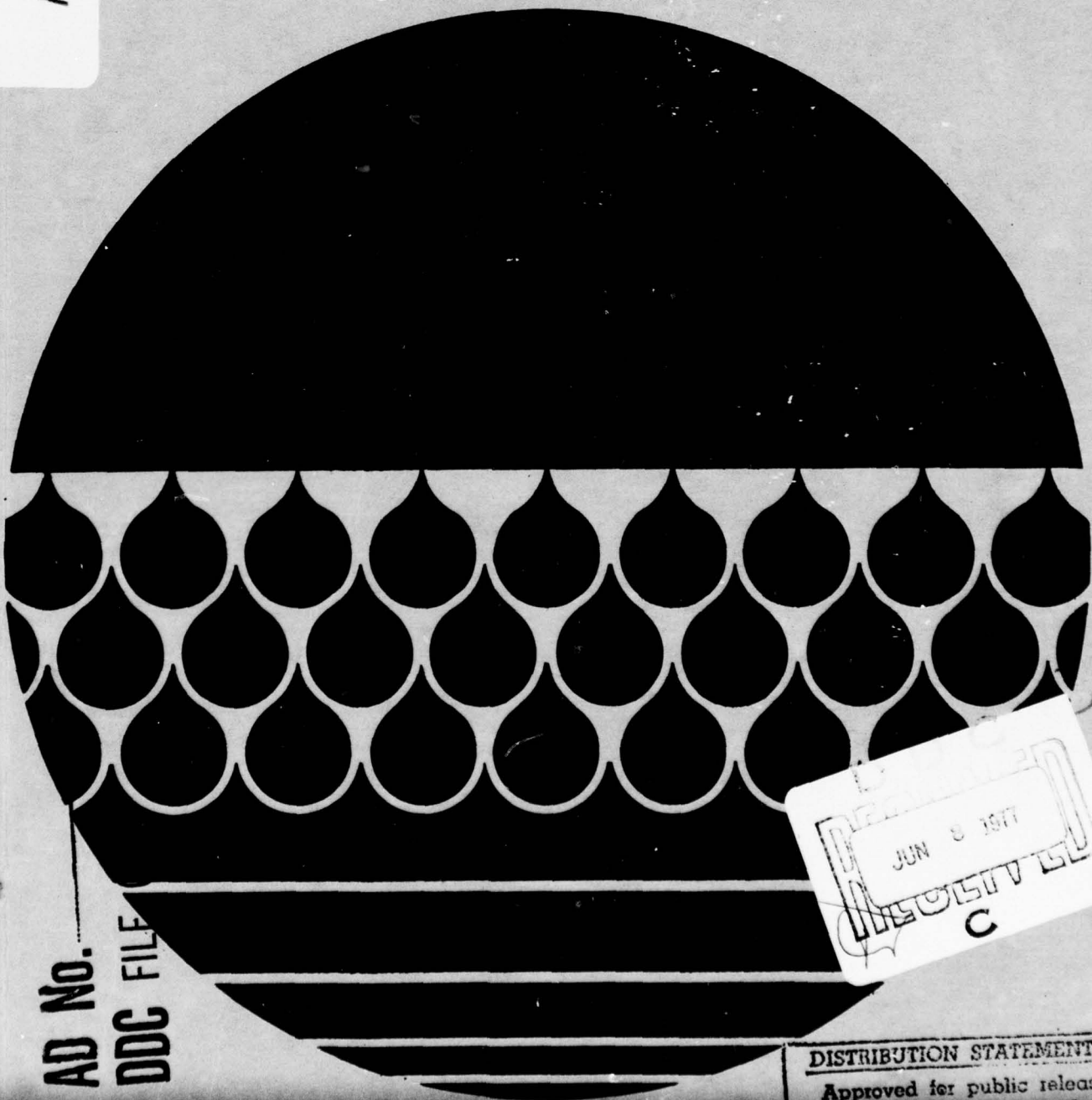
AD A 040299

Bedford Institute of Oceanography
L'Institut océanographique de Bedford

Dartmouth/Nova Scotia/Canada

A Comparison of the Air-Sea Interaction Flux Measurement Systems of the
Bedford Institute of Oceanography and the Institute of Oceanography,
University of British Columbia

S. D. Smith, R. J. Anderson, E. G. Banke, E. P. Jones, S. Pond, & W. G. Large
Report Series/BI-R-76-17/ December 1976



AD No.
DDC FILE



DISTRIBUTION STATEMENT A
Approved for public release;
Distribution Unlimited

The Bedford Institute of Oceanography is a Government of Canada establishment whose staff undertake scientific research and surveys in the marine environment. It consists of three main units: (1) the Atlantic Oceanographic Laboratory, which is part of Fisheries and Marine Service, Department of the Environment, (2) the Marine Ecology Laboratory, also of Fisheries and Marine Service, Department of the Environment, and (3) the Atlantic Geoscience Centre of the Geological Survey of Canada, Department of Energy, Mines and Resources.

L'Institut océanographique de Bedford est un établissement du gouvernement du Canada, dont le personnel entreprend des travaux de recherche scientifique et des études se rapportant au milieu marin. Il comprend trois services principaux: (1) le Laboratoire océanographique de l'Atlantique, qui fait partie du Service des pêches et des sciences de la mer du ministère de l'Environnement, (2) le Laboratoire d'écologie marine, qui relève également du Service des pêches et des sciences de la mer du ministère de l'Environnement, et (3) le Centre géoscientifique de l'Atlantique de la Commission géologique du Canada, ministère de l'Énergie, des Mines et des Ressources.

UNCLASSIFIED

SECURITY CLASSIFICATION OF THIS PAGE (When Data Entered)

REPORT DOCUMENTATION PAGE		READ INSTRUCTIONS BEFORE COMPLETING FORM
1. REPORT NUMBER BI-R-76-17	2. GOVT ACCESSION NO.	3. RECIPIENT'S CATALOG NUMBER
4. TITLE (and Subtitle) A COMPARISON OF THE AIR-SEA INTERACTION FLUX MEASUREMENT SYSTEMS OF THE BEDFORD INSTITUTE OF OCEANOGRAPHY AND THE INSTITUTE OF OCEANOGRAPHY, UNIVERSITY OF BRITISH COLUMBIA.		5. TYPE OF REPORT & PERIOD COVERED Technical Report,
7. AUTHOR(s) S.D./Smith, R.J./Anderson, E.G./Banke, E.P./Jones, S./Pond & W.G. Large		6. PERFORMING ORG. REPORT NUMBER 45
9. PERFORMING ORGANIZATION NAME AND ADDRESS Institute of Oceanography University of British Columbia Vancouver, B.C., Canada V6T 1W5		8. CONTRACT OR GRANT NUMBER(s) N00014-76-C-0446 NR 083-207
11. CONTROLLING OFFICE NAME AND ADDRESS Office of Naval Research NORDA Code 410/ONR Code 481 Bay St. Louis, Mississippi 39520		10. PROGRAM ELEMENT, PROJECT, TASK AREA & WORK UNIT NUMBERS --
14. MONITORING AGENCY NAME & ADDRESS (if different from Controlling Office) 1249p.		12. REPORT DATE December 1976
		13. NUMBER OF PAGES 41
		15. SECURITY CLASS. (of this report)
		15a. DECLASSIFICATION/DOWNGRADING SCHEDULE
16. DISTRIBUTION STATEMENT (of this Report) Unlimited		
17. DISTRIBUTION STATEMENT (of the abstract entered in Block 20, if different from Report) ---		
18. SUPPLEMENTARY NOTES ----		
19. KEY WORDS (Continue on reverse side if necessary and identify by block number) Air-sea flux measurements system intercomparison		
20. ABSTRACT (Continue on reverse side if necessary and identify by block number) See reverse side.		

UNCLASSIFIED

SECURITY CLASSIFICATION OF THIS PAGE(When Data Entered)

20.

ABSTRACT

A comparison of two air-sea interaction measurement systems was run at Sable Island, N. S., in September and October, 1975. The BIO sensors included thrust and sonic anemometers for wind turbulence measurement, a microbead thermistor, and a Lyman-alpha humidity sensor. The UBC system consisted of a modified Gill propeller-vane anemometer, thermistors, and Brady and aluminum oxide type humidity sensors. Both data sets were recorded in fm analogue form and digitized and analyzed at BIO. The UBC system also made digital recordings, which will be reported elsewhere.

Both systems operated together to produce generally comparable results. A certain number of differences and problems are discussed.

UNCLASSIFIED

SECURITY CLASSIFICATION OF THIS PAGE(When Data Entered)

BEDFORD INSTITUTE OF OCEANOGRAPHY ✓

Dartmouth, Nova Scotia
Canada

A COMPARISON OF THE AIR-SEA INTERACTION

FLUX MEASUREMENT SYSTEMS OF THE

BEDFORD INSTITUTE OF OCEANOGRAPHY

AND THE

INSTITUTE OF OCEANOGRAPHY, UNIVERSITY OF BRITISH COLUMBIA

by

S.D. Smith, R.J. Anderson, E.G. Banke and E.P. Jones

Atlantic Oceanographic Laboratory
Ocean and Aquatic Sciences
Department of the Environment

and

S. Pond and W.G. Large


Institute of Oceanography, University of British Columbia
Vancouver, B.C.

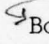
December 1976

REPORT SERIES


BI-R-76-17 ✓

ABSTRACT*(Bedford Institute of Oceanography)*


 A comparison of two air-sea interaction measurement systems was run at Sable Island, N. S., in September and October, 1975. The BIO sensors included thrust and sonic anemometers for wind turbulence measurement, a microbead thermistor, and a Lyman-alpha humidity sensor. The UBC system consisted of a modified Gill propeller-vane anemometer, thermistors, and Brady and aluminum oxide type humidity sensors. Both data sets were recorded in fm analogue form and digitized and analyzed *(University of British Columbia)* at BIO. The UBC system also made digital recordings, which will be reported elsewhere.


 Both systems operated together to produce generally comparable results. A certain number of differences and problems are discussed.

SOMMAIRE


 En septembre et octobre 1975, à l'île de Sable (N.-E.), on a procédé à la comparaison de deux systèmes de mesure de l'interaction atmosphère-mer. Les détecteurs de l'Institut océanographique de Bedford comprenaient des anémomètres soniques et de poussée destinés à mesurer la turbulence des vents, un micro-thermistor et un détecteur d'humidité Lyman-Alpha. Le système de l'Université de Colombie-britannique se composait d'un anémomètre Gill modifié, à hélice et girouette, de thermistors, et de détecteurs d'humidité de types Brady et à oxyde d'aluminium. Les deux séries de données ont été enregistrées de façon analogue, en FM, et analysées à l'Institut océanographique de Bedford. Le système de l'Université de Colombie-britannique a aussi fait des enregistrements numériques dont le rapport figurera ailleurs.

Les deux systèmes ont fonctionné ensemble pour donner des résultats comparables dans l'ensemble. Il est discuté dans le texte d'un certain nombre de différences et de problèmes.

A

CONTENTS

Abstract	-----	i
Contents	-----	ii
Symbols	-----	iii
1. Introduction	-----	1
2. Instrumentation	-----	2
3. Data processing	-----	6
4. Results	-----	7
4.1 Velocity	-----	7
4.2 The Drag Coefficient	-----	19
4.3 Spectra	-----	23
4.4 Temperature Fluctuations and Sensible Heat Flux	-----	29
4.5 Humidity	-----	35
5. Summary	-----	39
6. Acknowledgements	-----	40
7. References	-----	41

SYMBOLS

B_0, B_1, B_2, B_3	Coefficients of polynomial relating thrust anemometer signals to wind tilt in degrees.
$C_{10} = -\overline{u_1 u_3} / U_{10}^2$	Sea surface drag coefficient.
$C_T = \overline{tu_3} / U_{10} \Delta T$	Heat flux coefficient
$C_Q = \overline{qu_3} / U_{10} \Delta Q$	Evaporation coefficient.
f	Frequency
GMT	Greenwich Mean Time, 4 hours ahead of local Atlantic Standard Time.
Q	Mean water vapour density
q	Fluctuation in water vapour density.
$r_{13} = \overline{u_1 u_3} / \sigma_1 \sigma_3$	Correlation coefficient between downwind and vertical wind components.
T	Mean air temperature
t	Air temperature fluctuation
T_s	Sea surface ("bucket") temperature.
$\Delta T = T_s - T$	Temperature difference between sea surface and 10 m height.
U	Mean wind velocity.
U_{10}	Mean wind velocity at a height of 10 m above the surface
u_i	Wind velocity component.
$u_* = (-\overline{u_1 u_3})^{1/2}$	Friction velocity.
V_H	Horizontal velocity, in anemometer axes
W	Vertical velocity, in anemometer axes

$$\sigma_i = (\overline{u_i^2})^{1/2}$$

Standard deviation of velocity component.

$$\sigma_t, \sigma_q$$

Standard deviation of temperature, humidity.

$$\phi_{ij}(f)$$

Spectrum (if $i=j$), or cospectrum (if $i \neq j$)

$i=1,2,3$ (as subscript)

Downwind, lateral, and vertical components.

(The first axis is aligned with the mean wind.)

overbar

Average over a data run, typically of about
40 min duration.

1. INTRODUCTION

Air-sea interaction measuring systems have been designed and constructed at the Bedford Institute of Oceanography (BIO) and at the Institute of Oceanography, University of British Columbia (IOUBC) to measure wind velocities, humidity and temperature for determinations of momentum, moisture and heat fluxes between the ocean and atmosphere. Although the two systems are intended to measure the same physical quantities, they use different sensors and data acquisition systems. In addition, the analogue tape recorder in the BIO system has relatively high power consumption whereas the IOUBC system has very modest power requirements. Further, the IOUBC system records digitally in intermittent bursts to greatly reduce the quantity of tape required with the result that it can be self-contained, while for remote sites the BIO data must be recorded using telemetry.

An intercomparison experiment was conducted with the two systems in order to be able to compare future results, especially those to be obtained from a stable tower moored off Halifax Harbour. In the present experiment, data from both the BIO and IOUBC sensors were recorded on the BIO data recording system. The IOUBC system records will be compared to these results when the IOUBC analysis system development is completed.

The intercomparison study was made on Sable Island, Nova Scotia, from mid-September to the end of October 1975. Sable Island was chosen because it is a relatively convenient site for air-sea interaction studies and because earlier work had been done there with the BIO system (Smith and Banke, 1975). This earlier work was done on the west spit of the island, but, because reaching that site from the support facilities of the meteorological station was time consuming and sometimes impossible due to beach

conditions, a more convenient site on the south side of the island nearer the meteorological station was chosen for this work.

2. INSTRUMENTATION

The various sensors were mounted 10 to 13 m above the sea surface (depending on the tide) on a 9 m high mast located about 30 m from the water's edge (Fig. 1). The IOUBC digital recording system was mounted at the base of the mast and the BIO recording system was housed in a hut about 50 m inland from the mast.

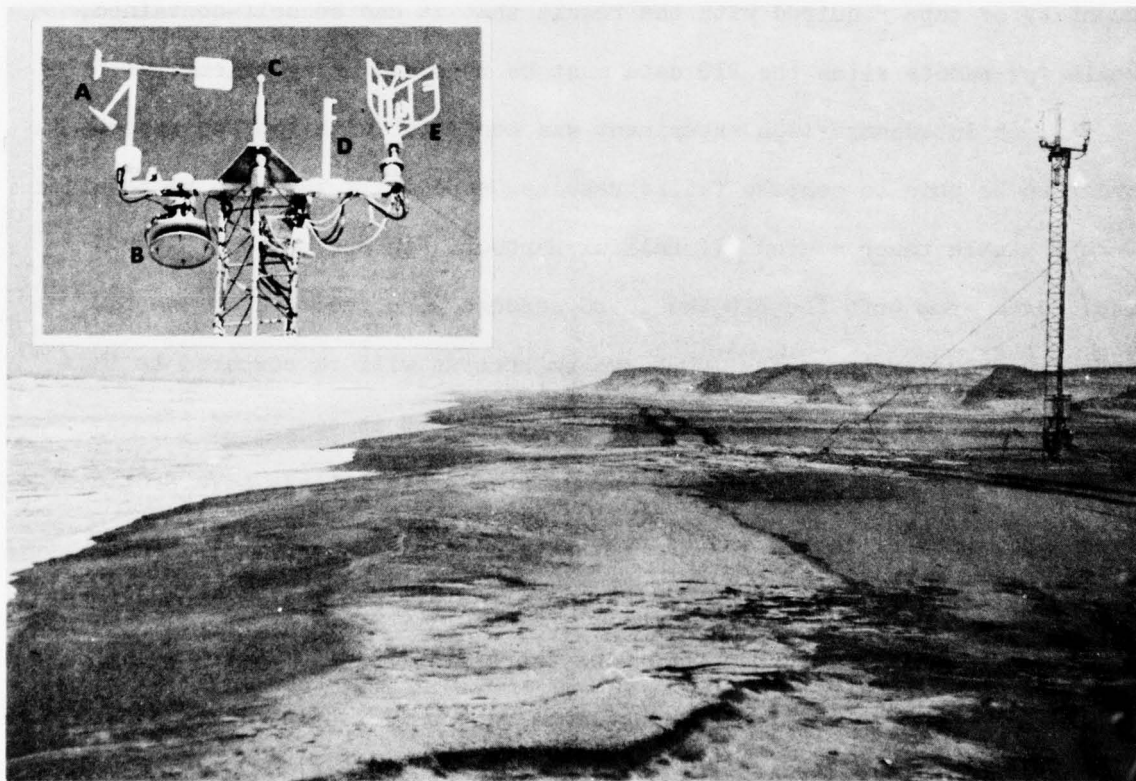


Figure 1. The instrument tower at low tide. The high water line can be seen half way up the beach. Inset - the sensors: (A) UBC Gill anemometer; (B) shield containing UBC temperature and humidity sensors; (C) BIO Mark 7 thrust anemometer; (D) mounting bracket for BIO Lyman-alpha humidimeter; (E) BIO sonic anemometer with thermistor attached.

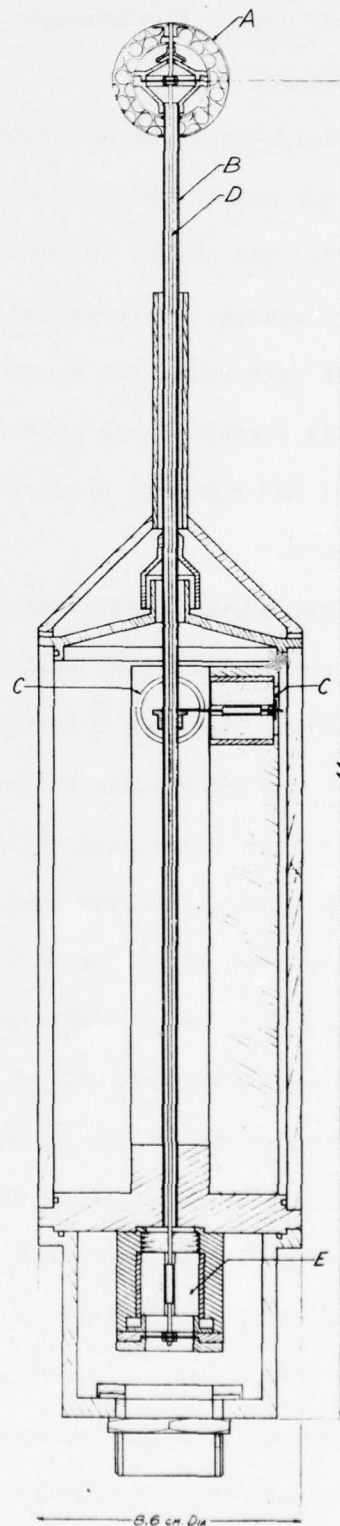
The BIO sensors consisted of a Kaijo-Denki PAT 311-1 sonic anemometer, two thrust anemometers, a Victory Engineering Corp. microbead thermistor, and an Electromagnetic Research Co. Model BLR Lyman-alpha humidity sensor.

The Kaijo-Denki three-component sonic anemometer has been widely accepted for measurements of atmospheric turbulence (Japan-U.S. Joint Study Group, 1971) and served in this experiment as a basis for comparison of the other anemometers. This anemometer has one failing: when the probes become wet from rain, the sound pulses are not always detected properly and the signals contain large spikes. In addition it requires frequent adjustment and consumes about 100 W, and so will not be used on the stable tower.

The two thrust anemometers measure three components of wind thrust on a perforated ping-pong ball using spring linkages and differential transformers. The Mark 6 design (Smith, 1969) has been in use for some time. Its spring linkage suffers from thermal drift, and from cross-coupling of the three axes which introduces errors up to 3° in indicated wind direction. The anemometer used was the fourth one built to this design and will be referred to as Thrust 6.4. Thermal drift can be essentially eliminated by recording zero-wind signals immediately before and after each data run and by the removal of linear trends from the data. Some of the cross-coupling errors can be compensated for in the data processing, but variations in cross coupling with wind thrust and direction cannot be eliminated entirely. The Mark 7 design, referred to as Thrust 7.1, has a simplified spring linkage (Fig. 2) with reduced cross-coupling introducing a smaller error, about 1° , in the indicated wind direction. It lacks the counterbalancing against horizontal acceleration of the Mark 6 and so is more prone to errors caused by movements or vibrations of its supporting mast. Because of this problem, which was very apparent in

Figure 2. Mark 7 thrust anemometer.

Horizontal wind thrust on sphere (A) deflects the outer tube (B) and is sensed by differential transformers (C). Vertical thrust moves the inner tube (D) and is sensed by a differential transformer (E).



the Sable Island measurements, the development of the Mark 7 anemometer has been discontinued. It remains a usable instrument if mounted on a very solid tower.

The BIO microbead thermistor (Thorpe, 1973) was exposed to the air stream in a small (25 mm diameter) radiation shield mounted near the sonic anemometer probe.

The Lyman-alpha humidimeter was operated with an absorbing path length of 0.5 cm and a source current of 50 μ A. Calibration was achieved by placing it in an enclosed box with a psychrometer and a Cambridge Systems Model 137 dew point hygrometer. A number of calibration points over a small range of absolute humidity was obtained in this manner and the ambient humidity reading was checked with a psychrometer on the tower before each data run. Some drift did occur. Because the humidimeter was exposed to the air flow with no weather shield and was vulnerable to moisture damage, it was mounted on the tower only during some data runs.

The BIO data were recorded on IRIG (Intermediate Range Instrumentation Group) frequency-multiplexed channels 1 to 12 using a Crown Model CI 822 tape recorder running at $7\frac{1}{2}$ inch/s. A 14.5 kHz reference tone was added to the signal to allow compensation during playback for tape speed variation.

The IOUBC system measured wind velocities with a modified Gill anemometer (R.M. Young & Co., Traverse City, Michigan, U.S.A.) which has the standard propeller vane unit and a lengthened vertical shaft. A second propeller was added with its axis pointing downward at an angle of about 30° from the vertical instead of pointing vertically upward as is more usual. The non-vertical axis avoids the stalling and non-linear response common in the usual configuration for vertical wind velocities less than $\frac{1}{2}$ m/s; The tilted propeller ensures that it always operates above the threshold and non-linear regions for wind speeds above 3 m/s. The second propeller thus measures a combination of the horizontal component of

the wind velocity, V_H , and the vertical component, W , but it does not follow a cosine law exactly and a more complicated calculation is required to extract W from the two propellers.

The IOUBC system also has a microbead thermistor (Victory Engineering Corp.) for temperature measurements, a glass rod thermistor to measure sea temperature which in this experiment was used to check the microbead thermistor, a Brady array (Thunder Scientific Inc.) for relative humidity measurements and an aluminum oxide sensor (Panametrics Inc.) for absolute humidity measurements. The temperature and humidity sensors were mounted in a protective shield of the size and shape of a sombrero (inset in Fig. 1). The IOUBC sensors, the method to obtain u_3 from the Gill anemometer, the IOUBC dissipation method and eddy-correlation method recording packages will be described elsewhere (Pond and Large, 1977).

3. DATA PROCESSING

The analogue data tapes were digitized at the BIO Computing Centre using Program A TO D (Smith, 1974). This program linearized the thrust anemometer and BIO thermistor output, converted the sonic anemometer data to orthogonal coordinates, and used range and offset values to convert data from linear sensors to physical units. In a second pass through the data the program removed means and linear trends, rotated coordinates from the anemometers into coordinates aligned with the indicated mean wind direction so that the vertical and cross-stream wind components had zero means, and wrote the data on magnetic tape for further analysis. The mean, rms, maximum and minimum values and the trends were printed, as well as the momentum and heat fluxes and the drag coefficient for a wind extrapolated to a height of 10 m above the surface. The extrapolation, which assumes wind velocities vary logarithmically with height, introduced small corrections and negligible errors in the 10 m wind velocity values, U_{10} .

A subroutine (GILL) was added to process the data from the UBC Gill three-component anemometer, and a small number of associated changes were made in the main program.

Our spectral analysis programs (Dobson *et al.*, 1974) read data from program A TO D, which removes means and trends. Detrending removes some of the variance associated with periods longer than the run length. This slightly reduces the downwind turbulence levels which we report, but the part which is removed was not adequately sampled in the first place. The effect on vertical winds and hence the turbulent fluxes is negligible. The highest frequency analysed, 5 Hz, is determined by the sampling rate of 10 per second. The lowest frequency, 0.005 Hz (sometimes 0.01 Hz), is determined by the length of blocks of data used in the spectral analysis.

Dubious data have been deleted from the results presented here (Table 1). The sonic anemometer tended to mistrigger in damp weather causing 'spikes' in the output which led to rejection of a number of data runs. The Mark 7 thrust anemometer suffered a connector failure, thus missing the first nine runs. Runs 16 and 35 were not digitized because they were recorded when the wind was blowing down off the dunes. Other reasons for deletions included excessive vibration of the thrust anemometer or signals running off-scale.

4. RESULTS

4.1 Velocity

The sonic anemometer will be the basis for comparison of results because it is more widely used, has a linear response which permits straightforward data processing, and has a flat response over our frequency range 0 to 5 Hz.

TABLE 1

SUMMARY OF WIND DATA

Run*	Time GMT	Date 1975	Duration min	V_{10} m/sec	From deg.	σ_1/U	σ_2/U	σ_3/U	σ_3/u_*	$-T_{13}$	$10^3 C_{10}$
2U	1359	27/9	44	6.37	225	0.057	0.027	0.026	0.95	0.42	0.85
3S	1502	27/9	39	5.91	225	0.033	0.052	0.044	1.29	0.33	1.13
3U	1642	27/9		6.80		0.069	0.054	0.026	0.97	0.39	0.80
4S				7.21	164	0.111	0.056	0.045	1.33	0.23	1.12
4U				7.53		0.111	0.063	0.030	1.03	0.27	1.07
5S	1801	27/9	42	7.05	225	0.087	0.063	0.041	1.32	0.27	0.93
5U				7.23		0.092	0.055	0.028	0.96	0.32	0.95
6S	1422	6/10	40	7.54	248	0.089	0.076	0.051	1.13	0.36	1.27
7S	1520	6/10	42	7.31	248	0.102	0.038	0.044	1.17	0.34	1.41
7U				8.06		0.101	0.079	0.036	0.90	0.40	1.32
8S	1632	6/10	43	8.46	248	0.083	0.065	0.044	1.30	0.30	1.15
8U				9.18		0.089	0.069	0.032	1.00	0.36	1.18
9S	1810	6/10	42	7.74	238	0.087	0.063	0.043	1.31	0.29	1.08
9U				8.42		0.085	0.064	0.031	1.00	0.37	1.16
10S	1339	12/10	43	9.83		0.092	0.062	0.042	1.25	0.30	1.14
10T				10.20	114	0.107	0.130	0.043	1.10	0.34	1.56
10U				10.32		0.094	0.066	0.029	1.03	0.29	0.94
11S	1502	12/10	42	11.06		0.088	0.059	0.043	1.23	0.32	1.20
11T				11.25	115	0.105	0.101	0.056	1.05	0.40	1.90
11U				11.58		0.091	0.065	0.030	0.94	0.37	1.16
12S	1628	12/10	42	10.33		0.089	0.060	0.047	1.24	0.35	1.41
12T				10.51	119	0.103	0.124	0.047	1.17	0.32	1.58
12U				10.89		0.089	0.062	0.032	0.99	0.37	1.25
13S	1739	12/10	43	11.10		0.096	0.057	0.045	1.28	0.32	1.22
13T				11.29	117	0.084	0.097	0.045	1.17	0.32	1.45
13U				11.55		0.087	0.062	0.031	1.01	0.35	1.11
14S	1859	12/10	43	12.02		0.091	0.070	0.047	1.21	0.35	1.49
14T				12.62	114	0.099	0.086	0.041	1.13	0.33	1.32
14U				12.71		0.091	0.076	0.032	0.96	0.39	1.31
15T	2002	12/10	43	12.90	113	0.103	0.124	0.045	1.21	0.30	1.39
15U				12.78		0.093	0.063	0.031	0.97	0.35	1.18
17S	1844	18/10	32	7.81	119	0.152	0.072	0.043	1.39	0.15	0.97
18T	1405	20/10	44	12.33	103	0.107	0.077	0.048	0.99 [†]	0.46 [†]	2.35 [†]
18U				12.65		0.093		0.033	0.89	0.43	1.58
19T	1500	20/10	44	12.34	108	0.093	0.078	0.044	1.04	0.41	1.79
19U				12.45		0.093		0.032	0.92	0.41	1.45
20T	1623	20/10	22	12.04	095	0.093	0.076	0.043	1.11	0.35	1.46

20U			12.44	0.051	0.029	0.88	0.43	1.31
21S	1300	20/10	44	12.03	0.053	1.22	0.31	1.51
21T				12.70	0.072	0.041	1.10	0.31
21U			108	12.81		0.032	0.89	0.40
22T	1930	20/10	44	13.94	0.053	0.042	1.05	0.34
23U				14.09	0.072	0.034	0.88	0.41
23T	2105	20/10	41	14.19	0.052	0.046	1.14	0.35
23U				14.54	0.066	0.034	0.89	0.43
24T	2215	20/10	41	15.12	0.069	0.045	1.08	0.37
24U				15.16	0.069	0.036	0.92	0.42
25T	0230	22/10	43	11.03	0.053	0.053	1.18	0.29
25U				12.02	0.078	0.036	0.98	0.34
29S	1213	22/10	44	9.61	0.074	0.044	1.31	0.35
29T				9.94	0.063	0.047	1.21	0.39
29U				9.94	0.076	0.034	1.00	0.45
30S	1316	22/10	44	9.31	0.072	0.050	1.36	0.33
30T				9.70	0.079	0.064	1.21	0.41
30U				9.56	0.074	0.034	1.06	0.42
31S	1408	22/10	44	8.93	0.070	0.049	1.34	0.35
31T				9.23	0.077	0.054	1.25	0.39
31U				9.10	0.072	0.054	1.08	0.41
32S	1612	22/10	44	9.19	0.073	0.051	1.41	0.30
32T				9.66	0.081	0.054	1.34	0.31
32U				9.57	0.073	0.054	1.07	0.39
33S	1500	22/10	44	11.09	0.082	0.053	1.33	0.32
33T				11.48	0.094	0.064	1.07	0.51
33U				11.70	0.082	0.057	1.01	0.42
34T	1704	22/10	44	10.90	0.092	0.059	1.14	0.41
34U				10.82	0.086	0.058	0.94	0.47
36S	1616	25/10	44	6.12	0.066	0.049	1.36	0.32
37S	1734	25/10	44	5.58	0.072	0.047	1.41	0.29
38S	1846	25/10	16	5.93	0.062	0.053	1.42	0.34
38U				6.16	0.061	0.030	0.98	0.51
* S-Sonic anemometer								
			Mean	0.057	0.059	0.043	1.30	0.30
			Standard deviation	0.019	0.010	0.002	0.08	0.08
			No. of runs	22	22	22	22	22
T-Thrust anemometer								
			Mean	0.100	0.082	0.046	1.15	0.35
			Standard deviation	0.015	0.023	0.004	0.08	0.04
			No. of runs	20	20	20	18	18
U-UBC Gill anemometer								
			Mean	0.089	0.065	0.032	0.97	0.39
			Standard deviation	0.013	0.010	0.003	0.06	0.05
			No. of runs	28	23	28	28	28

† Data not used in calculating mean and standard deviation.

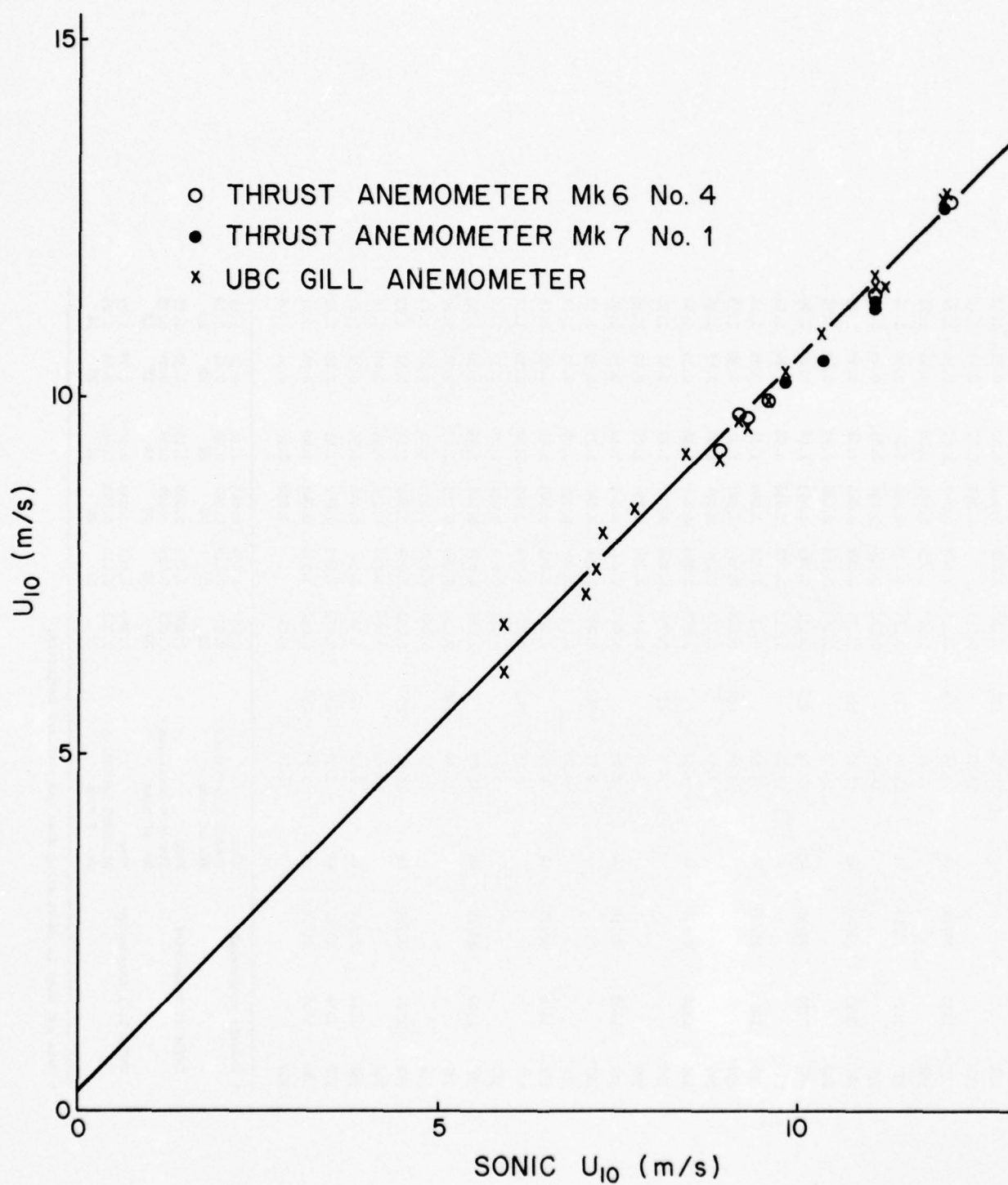


Figure 3. Comparison of mean wind speeds with regression line of U_{GILL} on U_{SONIC} .

Figure 3 shows the mean wind speeds from the Gill anemometer (U_{GILL}) $U_{\text{THRUST}} 7.1$ and $U_{\text{THRUST}} 6.4$ plotted versus U_{SONIC} . A linear regression for the average wind speed at 10 m, U_{10} , gives

$$(U_{10})_{\text{GILL}} = 1.02 (U_{10})_{\text{SONIC}} + 0.33 \text{ m/s.}$$

The sonic anemometer gives lower values for the mean wind speed than the Gill anemometer (Fig. 3). Calibrations of the sonic anemometer electronics by introducing measured delays in its sound pulses (Table 2) showed it to be within the manufacturer's $\pm 3\%$ specification of the factory values (3, 10, and 30 m/s full-scale for horizontal components and 1, 3, 10 m/s for vertical components) and so didn't change by more than 2% between calibrations.

The higher wind speeds indicated by the UBC Gill anemometer may be attributed to small errors in calibrating the anemometers and in setting the voltage corresponding to zero wind speed.

The Gill anemometer is calibrated by rotating the propeller shaft at known rates and measuring the output voltage. The conversion factor between rotation rate and wind velocity is supplied by the factory and, although not done for this particular anemometer, direct wind tunnel calibrations of Gill anemometers at UBC and elsewhere have always shown excellent agreement with factory calibrations (1-2%). Post-experiment calibrations confirmed the earlier ones within experimental error (about one part in 250). Uncertainty in the dc level at zero wind and in the offset are equivalent to 0.005 and 0.15 m/s respectively. The first could be systematic, while 0.1 m/s of the second is expected to be random. Thus, the Gill anemometer ought to indicate velocities that are at most 2% high.

TABLE 2

SONIC ANEMOMETER NO. 2 CALIBRATION

(FULL SCALE RANGE AT 20C)

PERFORMED BY TIMING PULSES

Range	(Before (09/09/75)*)			After (18/11/75)		
	A	B	W	A	B	W
	m/s	m/s	m/s	m/s	m/s	m/s
1	3.03	3.00	1.00	2.99	3.01	0.98
2	9.80	9.91	3.04	9.74	9.87	3.02
3	29.07	30.28	9.89	28.92	29.50	9.80

* These values used in data analysis.

The response of the Gill anemometer propellers falls off at high wave numbers, and is 3 dB down at a fluctuation wavelength of about 6 m. The turbulence scales (wavelengths) that contribute to the variances and covariances are proportional to height and at a fixed height are very nearly independent of wind speed. The reduction of measured variances and covariances due to anemometer response limitations is thus, fortunately, also independent of wind speed. At the height of observation, about 10 m, we expect the indicated covariance $\overline{u_1 u_3}$ to be about 85% of its true value. Examination of several cospectra $\phi_{13}(f)$ showed that for the Gill about 15% of the stress was lost due to small scale response limitations. Also, the stress from the Gill and Sonic agree on average if this condition is made and the calibration difference between the two instruments (discussed later) is taken into account. Since the BIO data processing system does not lend itself to making frequency-dependent corrections, we report indicated values for velocity fluctuation components keeping in mind that the vertical wind variance will be reduced. Corrected values of the covariance $\overline{u_1 u_3}$ are used in Table 1. While errors from either anemometer alone cannot account for the difference between the sonic and the Gill anemometers, the combined possible errors of the two anemometers can.

Thrust anemometer calibrations (Table 3) made before the experiment using the 200 ft field cable, and used in the analysis, indicated larger full-scale ranges (lower sensitivity) than calibrations made after the experiment without the long cable. The post-experiment calibration of Thrust 6.4 agrees within 1% in velocity with each of a series of seven calibrations from March to August 1974. The ranges of wind speeds observed with the thrust anemometers were not sufficient for regression analysis but the observed wind speeds agreed better with the Gill anemometer than with the sonic anemometer:

TABLE 3
THRUST ANEMOMETER CALIBRATION

Thrust Anemometer	Date	Range (m^2/s^2)			Relative Sensitivity		Vertical Angle Polynomial ⁺			
		0	1	2	3	$\frac{\text{Axis 1}}{\text{Axis 2}}$	$\frac{\text{Axis 1}}{\text{Axis 3}}$	B_0	B_1	B_2 B_3
6.4	*11/09/75	1847	938	484	262	1.149	0.2538	-4.6	69.6	72 -252
6.4	09/02/76	1682	850	429	211	1.147	0.2540	-3.9	71.7	-6 -104
7.1	*12/09/75	2287	1148	566	272	1.041	0.1346	-0.7	53.4	10 178
7.1	21/11/75	2137	1028	522	265	0.985	0.1342	-1.3	56.1	11 47

* These values used in data analysis.

+ Vertical wind angle in degrees, $\theta = B_0 + B_1 R + B_2 R^2 + B_3 R^3$ where R is ratio of vertical to horizontal thrust. The linear term $B_1 R$ is the dominant one.

$$U_{\text{THRUST } 6.4} / U_{\text{GILL}} = 0.990 \pm 0.027 \text{ standard deviation (12 runs)}$$

$$U_{\text{THRUST } 7.1} / U_{\text{GILL}} = 0.984 \pm 0.016 \quad (6 \text{ runs})$$

$$U_{\text{THRUST } 6.4} / U_{\text{SONIC}} = 1.042 \pm 0.009 \quad (5 \text{ runs})$$

$$U_{\text{THRUST } 7.1} / U_{\text{SONIC}} = 1.028 \pm 0.015 \quad (5 \text{ runs})$$

These results suggest that the Gill anemometer was reading slightly high (1 to 2%) while the sonic anemometer was slightly low (3 to 4%). Although the thrust anemometers are not necessarily more accurate than the others they were calibrated in a wind tunnel while the others were calibrated less directly, by timing of pulses (sonic) and by rotation rate (Gill anemometer). In preparation for the work on the stable platform, calibration of the Gill, thrust and Bendix Aerovane are being done in the wind tunnel at BIO to try to reduce calibration differences.

Comparing the standard deviation of downstream velocity σ_1 (Fig. 4) we see that the sonic anemometer generally indicates slightly lower levels than the Gill anemometer, by about the same amount as the difference in indicated mean wind.

The lateral response of the Gill anemometer is determined by the characteristics of the vane, which apparently tends to overshoot and increase the indicated turbulence levels by a further 5% (Fig. 5). Thrust anemometer 7.1 suffers badly from lateral vibration, while even thrust 6.4 which is counterbalanced against horizontal vibration gives σ_2 values some 15 to 20% higher than those from the sonic anemometer. The guy wires supporting the instrument mast were observed to sing in high winds and this appears to have had a detrimental effect on the thrust anemometers.

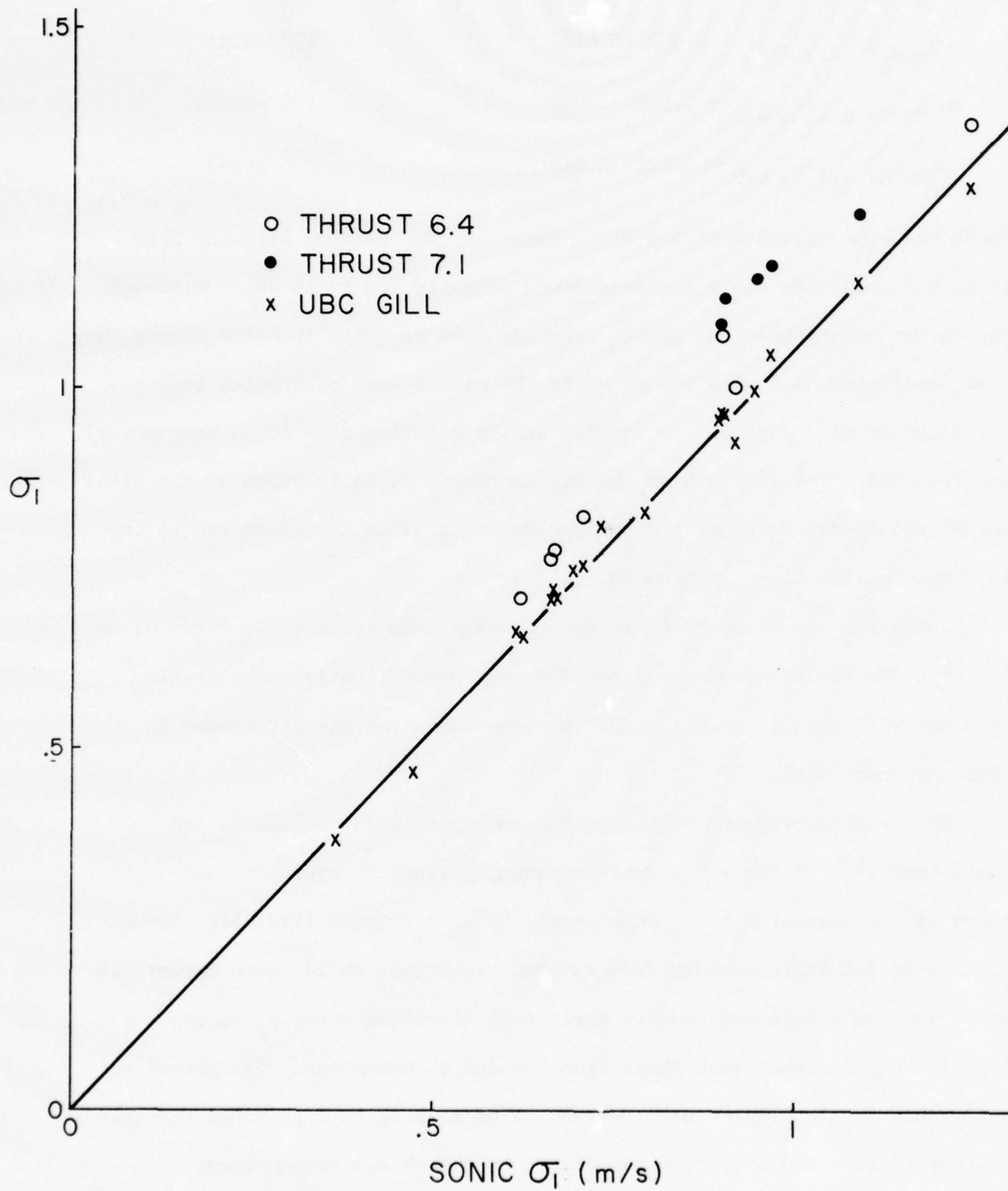


Figure 4. Comparison of downwind turbulence levels, with regression line $\sigma_1 \text{ GILL} = 0.002 \text{ m/s} + 1.058 \sigma_1 \text{ SONIC}$.

Vertical turbulence σ_3 indicated by the Gill anemometer is only about 75% of that indicated by the sonic anemometer (Fig. 6), as a result of attenuation of the smaller scales. Mounting the Gill anemometer on a higher tower, as was originally planned, would reduce this problem. As noted before the reduction is essentially independent of wind speed so a correction is easily made. Both thrust anemometers tend to give higher σ_3 values than the sonic anemometer by an amount comparable to the difference in indicated mean wind.

To test the ability of the anemometers to resolve whether the wind is relatively more or less gusty, we may compare the indicated turbulence levels divided by the mean wind speed. A linear regression from data in Table 1 gives very good agreement for the downwind component.

$$(\sigma_1/U_{10})_{\text{GILL}} = 0.003 + 0.97 (\sigma_1/U_{10})_{\text{SONIC}} \pm 0.003$$

correlation coefficient 0.96

The distribution of points and the above regression line are not the same as in Figure 4, since runs at higher wind speeds must have higher σ_1 values but need not have higher σ_1/U values. The thrust anemometers indicated higher levels with the mean ratio $(\sigma_1/U)_{\text{THRUST}}/(\sigma_1/U)_{\text{SONIC}}$ being 1.10 ± 0.04 and 1.13 ± 0.10 for Thrust 6.4 and Thrust 7.1 respectively.

In the lateral turbulence levels a similar pattern emerges, but the agreement is not quite so close, a regression line being

$$(\sigma_2/U)_{\text{GILL}} = 0.019 + 0.73 (\sigma_2/U)_{\text{SONIC}}$$

correlation coefficient 0.91

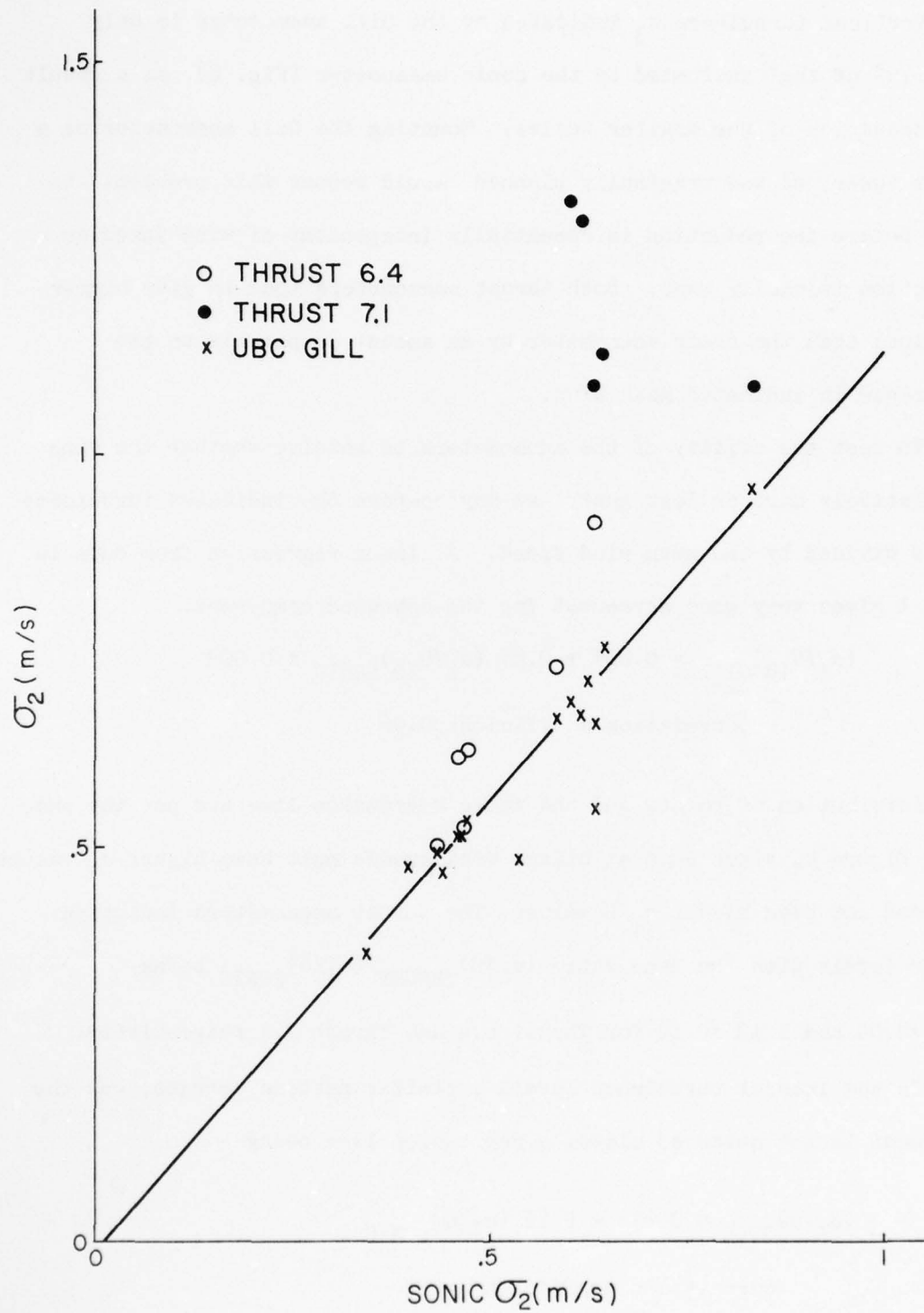


Figure 5. Comparison of cross-wind turbulence levels, with regression line $\sigma_2 \text{ GILL} = -9.013 \text{ m/s} + 1.143 \sigma_2 \text{ SONIC}$.

Thrust 7.1 suffered particularly badly from lateral vibration with the ratio $(\sigma_2/U)_{\text{THRUST}}/(\sigma_2/U)_{\text{SONIC}} = 1.76 \pm 0.35$ while for Thrust 6.1 the ratio was a more acceptable 1.21 ± 0.13 . The lateral turbulence is not required in our eddy flux calculations.

A linear regression comparison of vertical turbulence levels from Table 1 gives

$$(\sigma_3/U)_{\text{GILL}} = 0.011 + 0.48 (\sigma_3/U)_{\text{SONIC}} \pm 0.002$$

correlation coefficient 0.34

The first term (intercept) accounts for about one-quarter and the second term for about one-half of the rms vertical velocity indicated by the sonic anemometer, the remaining one-quarter being lost because of small-scale response limitation of the Gill anemometer. The correlation between Gill and sonic anemometers is not nearly so good for the vertical as for the downwind component, but this can be explained by the fact that σ_3/U varies less than the horizontal turbulence levels so that relatively small sensor variations become more apparent. The thrust anemometers agreed well with the sonic anemometer with ratios $(\sigma_3/U)_{\text{THRUST}}/(\sigma_3/U)_{\text{SONIC}}$ of 1.02 ± 0.09 and 0.99 ± 0.07 for Thrust 6.4 and Thrust 7.1 respectively.

4.2 The Drag Coefficient

The drag coefficient, $C_{10} = \overline{u_1 u_3} / (U_{10})^2$, where u_1 and u_3 are the downwind and vertical wind velocity fluctuations respectively, has been calculated for the four anemometers and is plotted in Figure 7. In this plot, values used in determining each C_{10} were obtained from the same instrument, so the effects of calibration differences between the instruments should be reduced. As noted earlier the values of $\overline{u_1 u_3}$ reported for the Gill have been corrected for its small scale response limitations by using originally calculated value divided by 0.85.

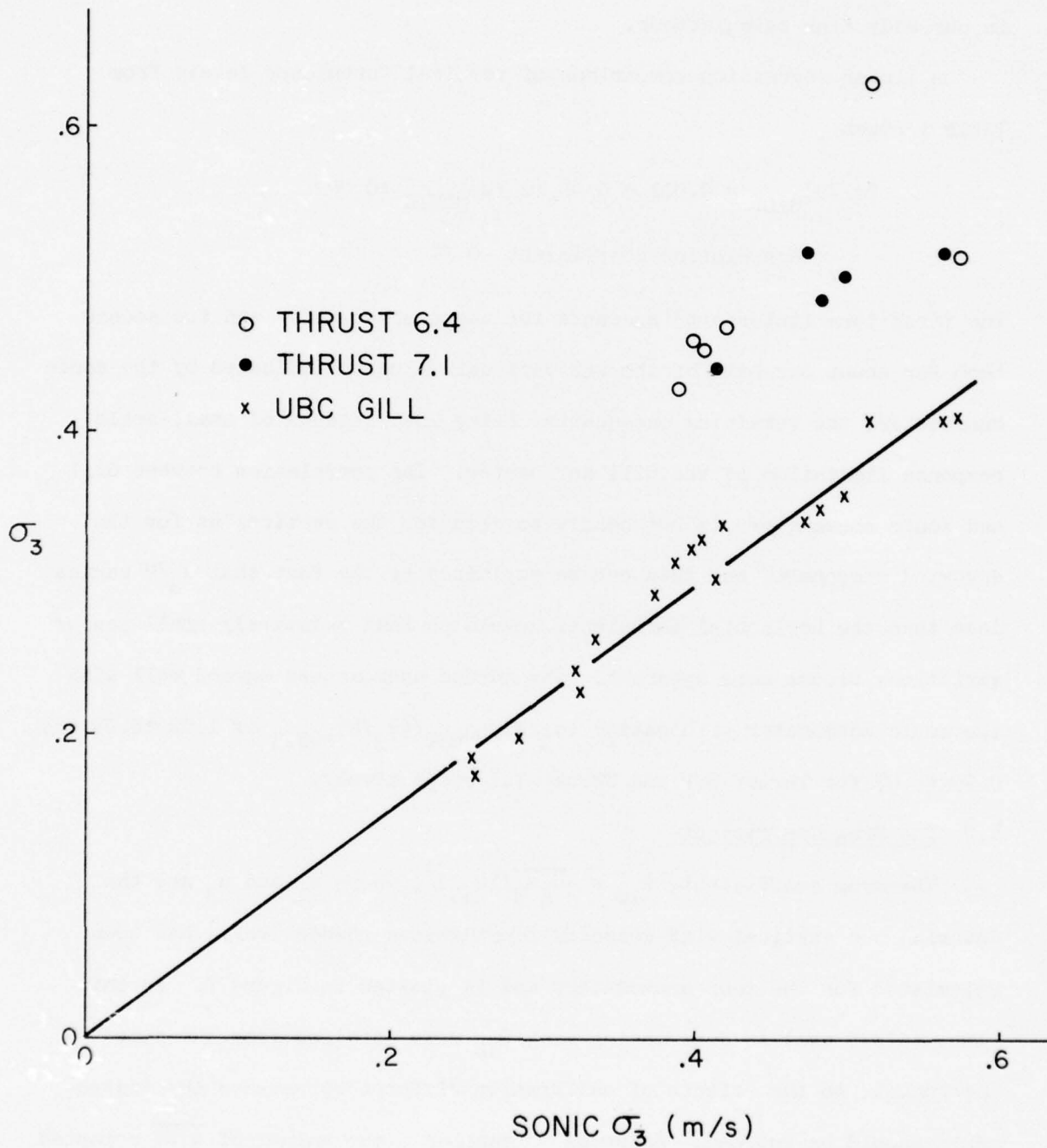


Figure 6.

Comparison of vertical turbulence levels, with regression
line $\sigma_3 \text{ GILL} = 0.002 \text{ m/s} + 0.745 \sigma_3 \text{ SONIC}$.

Although there is scatter, the results agree well on the whole. Since a possible error of 1° in the orientation of the coordinate system produces an error of 10% in the value of $\overline{u_1 u_3}$, for any one run values from two systems could easily differ by 20%. Detrending before calculating u_3 can also affect the u_3 and $\overline{u_1 u_3}$ values from the Gill anemometer. It appears that errors introduced by detrending when the trend and variation are large may cause low-frequency contributions to $\overline{u_1 u_3}$ GILL to be too small.

Least squares linear fits to the data for the drag coefficients from the sonic and Gill anemometers give

$$(10^3 C_{10})_{\text{SONIC}} = 0.59 + 0.063 (U_{10})_{\text{SONIC}}$$

$$(10^3 C_{10})_{\text{GILL}} = 0.41 + 0.083 (U_{10})_{\text{GILL}}$$

Because of the few points and small range of wind speed, regression line fits for the thrust anemometers were not warranted; however, as can be seen in Figure 7, the results are in reasonable agreement with those from the sonic and Gill anemometers. The overall result is consistent, considering scatter, with the relation $10^3 C_{10} = 0.63 + 0.066 U_{10}$ reported by Smith and Banke (1975).

The values for C_{10} averaged over all wind speeds, shown in Table 1, are not inconsistent with one another and with previous data (e.g. Smith and Banke, 1975). Much of the difference in values is associated with averaging over different runs. For 20 runs for which the Gill and sonic anemometers both give values, $10^3 C_{10} = 1.19 \pm 0.24$ and 1.18 ± 0.022 (mean \pm standard deviation) for Gill and sonic anemometers respectively. For 17 runs with Gill and thrust anemometers, the values are respectively 1.37 ± 0.25 and 1.49 ± 0.26 . For 11 runs with sonic and either of the thrust anemometers the values are 1.23 ± 0.24 and 1.41 ± 0.27 respectively. The thrust anemometer values are somewhat high, perhaps in part due to the

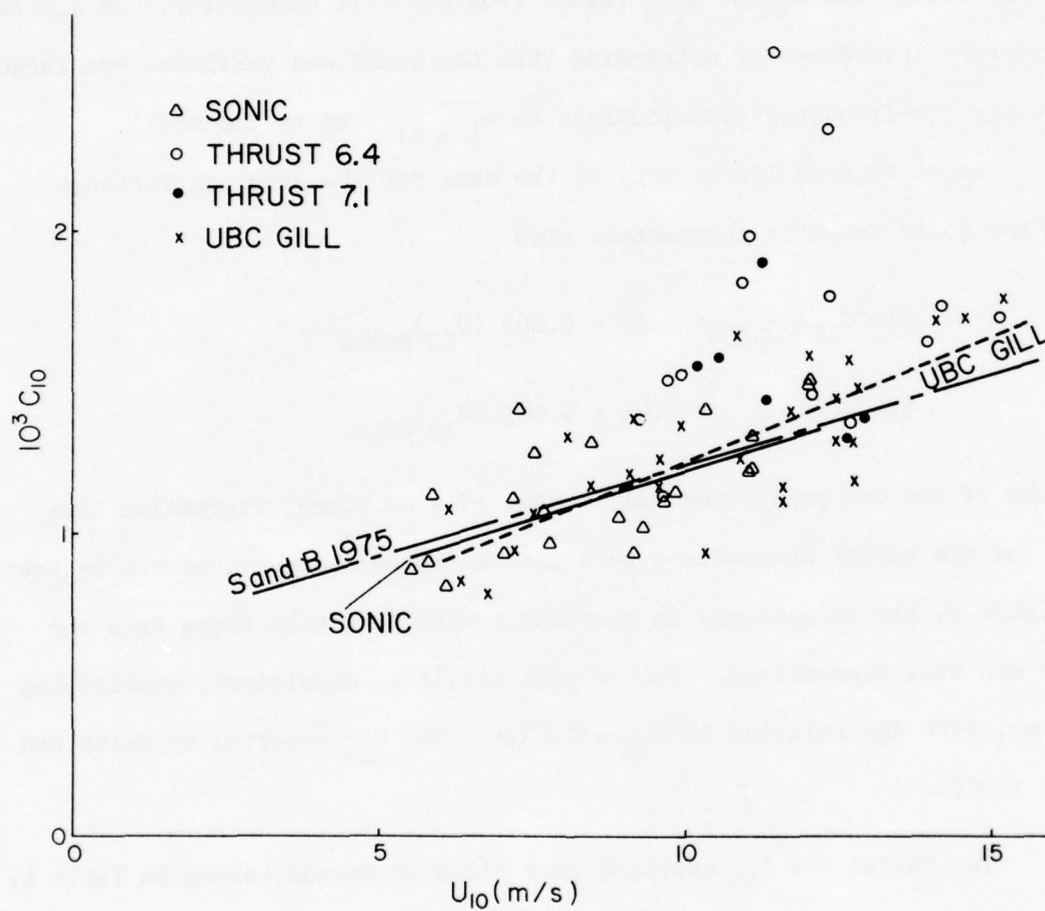


Figure 7. Drag coefficients plotted against wind speed with regression lines for Gill and Sonic and the regression line from Smith and Banke (1975).

vibration noise. Very high thrust anemometer drag coefficients for runs 18 and 33 were not used in calculating means and standard deviation.

The fact that not including a few runs can change C_{10} by 10 to 20% even when using the same site and instrument is worth noting. Much of the scatter in existing results and differences among them may be associated with having small samples of a variable process.

The values for σ_3/u_* and the overall correlation coefficients $-r_{13} = -\overline{u_1 u_3}/(\sigma_1 \sigma_3)^{1/2}$ given in Table 1 are within the usual range of values for turbulence in the lower boundary layer. Smith and Banke (1975), for example, found $\sigma_3/u_* = 1.2 \pm 0.1$ and $r_{13} = -0.34 \pm 0.07$. The Gill anemometer values are slightly different from the rest. Comparison with σ_3 SONIC and examination of ϕ_{33} spectra show that the Gill underestimates σ_3 by 25 to 30% because of its small scale response limitations. If we take the correct value to be $1.35 \sigma_3$ GILL then the average σ_3/u_* becomes 1.31 and the average $-r_{13}$ becomes 0.29, in much better agreement with values from the sonic and thrust anemometers. Note that in Table 1 $\overline{u_1 u_3}$ has been corrected for response limitations but σ_3 has not.

4.3 Spectra

Spectra and cospectra of the velocity, temperature, and humidity fluctuations have been analyzed over a frequency band from 0.005 Hz (sometimes 0.01 Hz) to 5 Hz. Logarithmically spaced bandwidths have been chosen. Examination of the spectra can reveal deficiencies of the sensors such as noisy operation or limited frequency response, since the general shapes of the spectra are well known from previous studies.

Velocity spectra for Run 32 are typical of data obtained with all three anemometers functioning well. The log-log plots (Fig. 8a,c,e) are useful for showing power-law spectral shapes as straight lines,

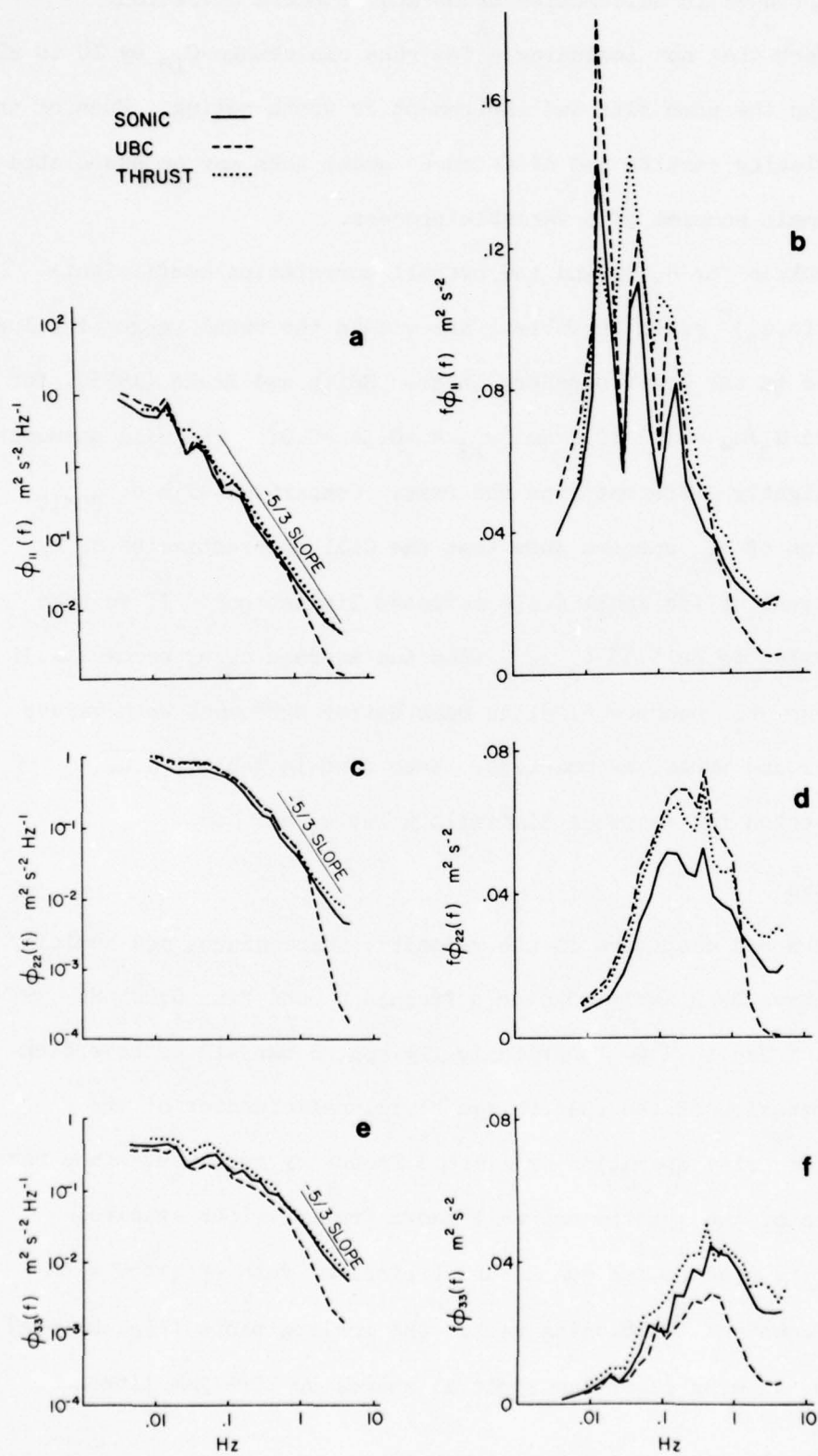


Figure 8. Velocity spectra for Run 32.

while plots of (frequency x spectrum) against logarithmic frequency (Fig. 8b,d,f) have areas proportional to kinetic energy and so give a better indication of the relative importance of spectral features. The downwind velocity components (Fig. 8a,b) show reasonable agreement, with the UBC Gill anemometer spectrum lying between the other two except above 0.5 Hz where its frequency response falls off. Different frequency bands were chosen for the thrust anemometer, giving slightly different relative sizes of small peaks within the spectrum. The expected $-5/3$ slope is seen in the log-log plot from 0.2 Hz to 2 Hz in the thrust and sonic anemometer spectra, while 'aliasing' of higher-frequency signals increases the computed spectra at frequencies around 3 to 5 Hz. The Gill anemometer spectrum has a slope of $-5/3$ over a relatively small range from 0.2 to 0.5 Hz.

The lateral or crosswind spectra (Fig. 8c,d) show better agreement in small peaks and valleys since all three were analyzed with the same array of bandwidths. The UBC Gill anemometer spectrum is higher than the others in the range 0.1 to 1 Hz, possibly due to overshooting of its direction vane, while its response falls off rapidly above 1 Hz. The thrust anemometer gives higher values than the sonic at all frequencies. All the spectra have a very small peak near 1 Hz which may be due to vibration of the tower.

In the vertical direction (Fig. 8e,f) the response of the UBC Gill anemometer is 3 dB down at a frequency of about 1 Hz, accounting for the lower values of σ_3 mentioned earlier. The sonic anemometer spectrum shows a $-5/3$ power law for a small range of frequencies around 1 Hz but this behavior is not nearly as well defined as for the downwind component. The range of frequencies analyzed barely reaches the area where local isotropy and the associated $f^{-5/3}$ power law behavior is possible. The observed spectra generally follow the expected shape. At 1 Hz the ratios $\phi_{33}(f)/\phi_{11}(f)$

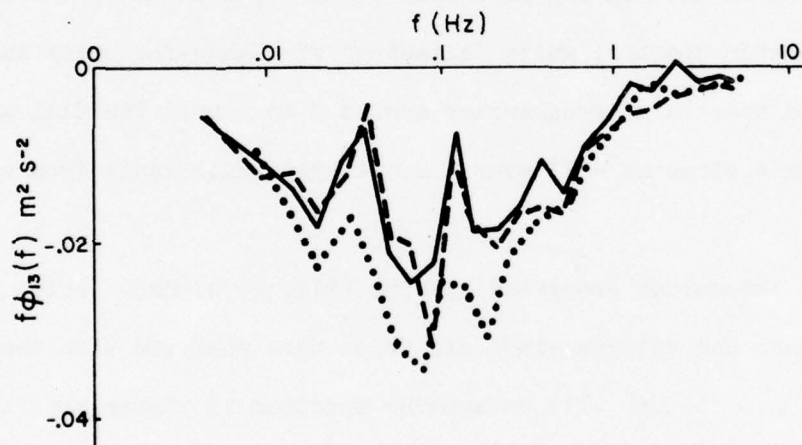


Figure 9. Wind stress cospectra for Run 32.
Sonic anemometer (solid line), Gill anemometer (dashed line), and thrust anemometer (dotted line).

for the sonic and thrust anemometers are 1.36 and 1.14 respectively for this run. Local isotropy theory predicts that this ratio should approach $4/3$ at the higher frequencies.

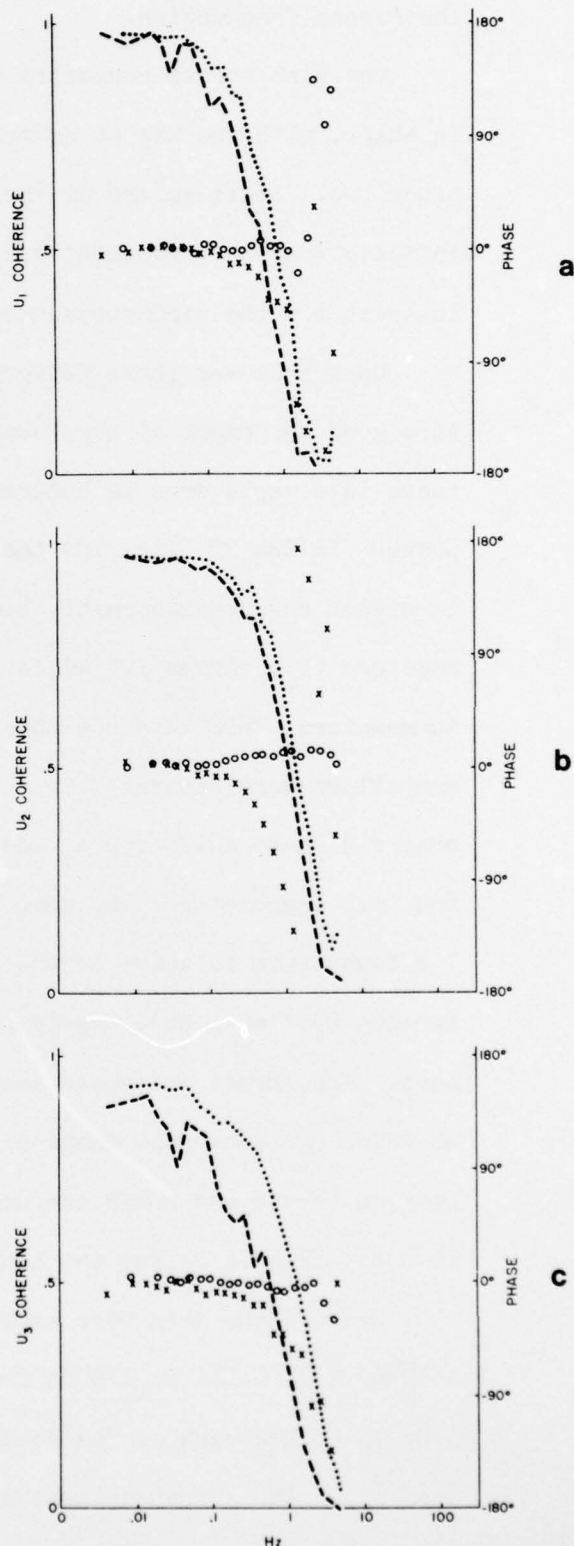
The wind stress cospectra $\phi_{13}(f)$ (Fig. 9) show general agreement in shape, with the thrust anemometer indicating higher stress than the other two. Small values at the low and high frequency end of the cospectrum indicate that the frequency band analyzed contains most of the range of interest for the wind stress measurement.

Coherence and phase between measurements of the velocity components show good agreement at the lower frequencies, but at higher frequencies there is a rapid drop in coherence accompanied by a more gradual shift in phase. In Run 32 (Fig. 10) the thrust-sonic anemometer coherence persists to higher frequencies partly because the separation between these two anemometers (1 m versus 1.7 m) is less than that of the UBC Gill and sonic anemometers. For this run the sonic and thrust anemometers and the UBC Gill propellers were separated in a nearly crosswind direction. Nearly all of the observed phase shift for u_1 and u_3 is due to the response characteristics of the Gill anemometer. The vane from which u_2 GILL is calculated is almost 1 m downstream relative to the sonic and so of the observed u_2 phase difference (90° at 1 Hz), nearly half (40° at 1 Hz) may be due to this displacement. The thrust and sonic anemometers remain in phase ($\pm 10^\circ$) up to frequencies at which the coherence drops to small values. The half-coherence frequency between thrust and sonic anemometers is lower for the downwind component (0.8 Hz) than it is for the lateral and vertical components (1.5 Hz).

Because the data were sampled 10 times per second, but low-pass filtered only by 3 db at 11 Hz (18 dB per octave rolloff), energy at frequencies above 5 Hz is folded back of "aliased" into the 5 Hz band covered by the spectral analysis. The thrust anemometers were particularly noisy at high frequencies, and aliasing may explain their generally higher spectral levels.

Figure 10.

Coherence spectra for Run 32 between UBC Gill anemometer and sonic anemometer (dashed line) and between thrust anemometer and sonic anemometer (dotted line). Phase, relative to sonic anemometer, of UBC Gill anemometer (X) and of thrust anemometer (O). (a) downwind, (b) cross-wind, and (c) vertical.



4.4 Temperature Fluctuations and Sensible Heat Flux

The mercury thermometer readings for air temperature, T , (Table 4) were taken near the top of the tower either before or after recordings. Thus in addition to reading error of ± 0.1 to 0.2°C there is uncertainty because they are not averages over the run as are the microbead values. Since σ_t is of the order of $0.1|\Delta T|$, the difference between instantaneous and mean temperatures could easily be $\pm 0.2 \Delta T$. This estimate is based on the assumption of Gaussian statistics and no large trends. Some of the differences between the mercury thermometer and the microbead values could be due to these errors.

Allowing for $\pm 0.5\%$ of full-scale nonlinearity or drift, the BIO thermistor should have an accuracy of $\pm 0.4^\circ\text{C}$. The mean temperature from the BIO thermistor agreed within 1°C with the mercury thermometer readings (Table 4) except for runs 28, 29 and 30 where the BIO thermistor behaved erratically, as will be discussed later.

When it is working properly the UBC thermistor should give an average air temperature to $\pm 0.2^\circ\text{C}$. The UBC thermistor and the mercury thermometer agreed within 0.3°C for the first few runs (2, 6, 7, 8 and 9 in Table 4), while afterward the differences were generally larger than 1°C . If the mean is not correct the fluctuations may also have some errors. We suspect shunting of the bead by salt films and in future shall insulate the leads and have a glass rod thermistor near the microbead to check it.

A water sample was taken from the surf with a bucket and T_s obtained from it with a reading error of $\pm 0.2^\circ\text{C}$. Thus the errors in T are perhaps $\pm 0.3^\circ\text{C}$ from reading plus 20% from sampling and are quite large.

Comparing the $\sigma_t/\Delta T$ values from the two systems, we see that the UBC values are smaller. Negative values are for cases with negative ΔT . When $|\Delta T| \leq 0.5^\circ\text{C}$ (runs 9, 11, 12, 23, 28 and 31) the standard deviation of temper-

TABLE 4
TEMPERATURE DATA

Run	Thermometer		Sonic	Gill	BIO Thermistor			UBC Thermistor		
	T C	Ts C			T C	$\frac{\sigma_t}{\Delta T}$ (or σ_t)	$\overline{u_3 t}$ C m/s	T C	$\frac{\sigma_t}{\Delta T}$ (or σ_t)	$\overline{u_3 t}$ C m/s
2	18.0	16.6	-	-8.9	17.2	-0.14	-0.009	18.0	-0.12	0.000
6	13.5	14.0	3.8	-	12.9	0.24	0.013	13.3	0.14	-
7	13.2	14.0	5.8	6.4	13.0	0.51	0.012	13.4	0.10	0.005
8	13.3	14.0	5.9	6.4	13.2	0.20	0.019	13.6	0.11	0.008
9	13.7	13.8	0.8	0.8	13.6	(0.16)	0.013	14.0	(0.11)	0.006
10	12.5	11.5	-9.8	-10.3	11.8	-0.08	0.009	13.8	-0.08	0.006
11	12.3	12.2	-1.1	-1.2	11.9	(0.08)	0.012	14.4	(0.08)	0.006
12	12.6	12.3	-3.1	-3.3	12.1	(0.09)	0.007	15.1	(0.07)	0.004
13	12.8	12.3	-5.5	-5.8	12.6	-0.12	0.007	15.2	-0.06	0.003
14	13.0	12.2	-	-10.1	12.5	-0.08	0.007	15.4	-0.06	0.005
15	12.6	12.1	-	-6.4	12.6	-0.12	0.007	15.8	-0.07	0.003
18	9.6	10.7	-	13.8	9.5	0.23	0.046	8.3	0.15	0.029
19	10.0	11.1	-	13.6	9.8	0.32	0.043	8.7	0.14	0.024
20	10.0	11.2	-	14.8	9.4	0.26	0.034	9.0	0.11	0.020
21	10.8	11.3	6.0	6.4	9.8	0.74	0.026	9.4	0.22	0.018
23	11.2	11.0	-	-2.9	10.8	(0.30)	0.009	9.8	(0.09)	0.008
24	11.2	11.0	-	-3.0	-	-	-	9.3	(0.06)	0.008
28	12.0	11.6	-	-4.8	10.4	(0.10)	-	9.8	(0.05)	0.001
29	12.3	12.0	-2.9	-3.0	11.1	-	-0.006	10.2	(0.04)	-0.001
30	12.6	12.0	-5.6	-5.7	11.3	-0.10	-0.002	10.3	-0.05	-0.001
31	12.6	12.0	-5.3	-5.4	11.7	-0.06	-0.003	10.4	-0.04	-0.001
33	12.7	12.2	-5.5	-5.8	13.0	-0.10	-0.005	10.4	-0.06	-0.002

Note: σ_t (C) is given in brackets in place of $\sigma_t/\Delta T$ in cases where $|\Delta T| \leq 0.5C$

ature σ_t is listed in Table 4 with brackets to allow comparison of values from the two systems. The $\sigma_t/\Delta T$ values are not nearly so uniform as those for wind components. Much of this scatter could be associated with the errors in ΔT . Because of the small ΔT 's the signals are small and there may be some noise included. Finally, there are some cases where one or the other system is not working properly. For example, the BIO thermistor data for Run 21 are dubious since large indicated fluctuations of 3- to 5-minute periods were not corroborated by the UBC thermistor. These fluctuations showed up as a large value of $\sigma_t/\Delta T$ (0.74), high spectral values at low frequencies, and reduced coherence at low frequencies between the BIO and UBC thermistors. This phenomenon persisted through Run 24, followed by excessive drift of the BIO thermistor during Runs 25 and 26. Rain fell during Runs 23 to 26, and a possible explanation of this peculiar behavior is salt or moisture contamination of the BIO thermistor bead.

Even though the microbeads are similar, an examination of the temperature spectra (Fig. 11a) shows higher values for the BIO thermistor at all frequencies. At high frequencies the values of the UBC thermistor fall off more rapidly and its phase lags the BIO thermistor (Fig. 11b). This is probably due to the shield which kept the UBC sensors out of the direct airflow. The sensor location has been changed to improve this response in future measurements. The shield may also contribute to the general lower ϕ_{tt} and $\sigma_t/\Delta T$ values of the UBC thermistors. However, it may be that the BIO thermistor values, particularly the peak at .03 Hz, are too high. A possible cause is occasional small step changes in the servo-potentiometer which balances out the mean temperature. As previously mentioned, salt or moisture contamination of one or both of the thermistor beads is always possible and could also have contributed to these effects.

Error bars in Fig. 11a give 90% confidence intervals for the spectral estimates and are generally similar to the error bars (not shown) for spectra of other variables in this paper.

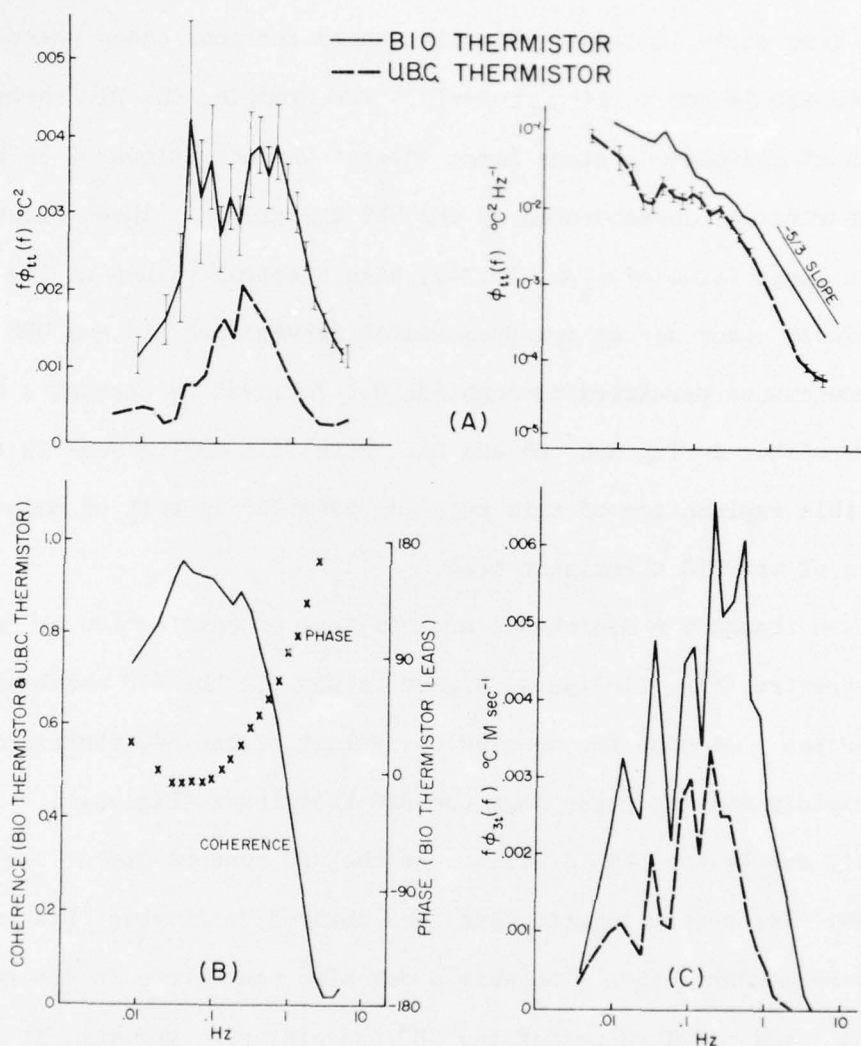


Figure 11. (a) Thermistor spectra for Run 8; BIO (solid), UBC (dashed).
 (b) Coherence and phase between UBC and BIO thermistors.
 (c) Heat flux cospectra for Run 8; BIO thermistor and sonic u_3 (solid), UBC (dashed).

Even if the σ_t values are affected by noise it may still be possible to measure the covariance $\overline{u_3 t}$ (e.g. Run 23, Table 4) since the noise in the two channels probably has a low correlation. Some of the recording noise, that associated with tape speed variation, will be correlated; compensation is done to reduce this noise but it cannot be eliminated entirely.

Figure 12a shows $\overline{u_3 t}$ from the two systems plotted against one another. These values, taken from Table 4, have not been corrected for sensor response limitations. Most of the values are fairly small but there does seem to be a consistent relationship particularly for the larger values. It appears that $(\overline{u_3 t})_{\text{UBC}} \approx 0.6 (\overline{u_3 t})_{\text{BIO}}$. Much of this difference is probably due to the response limits of the UBC sensors although some of it may also be due to calibration errors and noise.

Figure 12b shows $\overline{u_3 t}$ from each system plotted against $U\Delta T$ with U from the same system and ΔT from the mercury thermometer observations as noted before. There is a great deal of scatter which is caused by such things as the large possible errors in ΔT values and the small values of $\overline{u_3 t}$ leading to possible noise problems. The slopes of the regression lines are 1.3×10^{-3} and 1.0×10^{-3} for the BIO and UBC data sets, respectively. Most of this difference is probably due to response limitations noted before; a correction based on the slope of Figure 12a would give a slope of 1.7×10^{-3} for the UBC data. Both sets of data show an upward flux $\overline{u_3 t} = 0.0095 \text{ C m/s}$ (BIO) and 0.0076 C m/s (UBC) at $U\Delta T = 0$ which may be caused by the scatter, ΔT errors, noise, or may be real.

The slopes of the regressions are consistent with recent observations of $C_T = [\overline{u_3 t}/(U\Delta T)]$ reported by Friehe and Schmitt (1976) although, in view of the small values of $\overline{u_3 t}$ and the scatter, our values cannot be considered very reliable. However, the temperature fluctuations are small

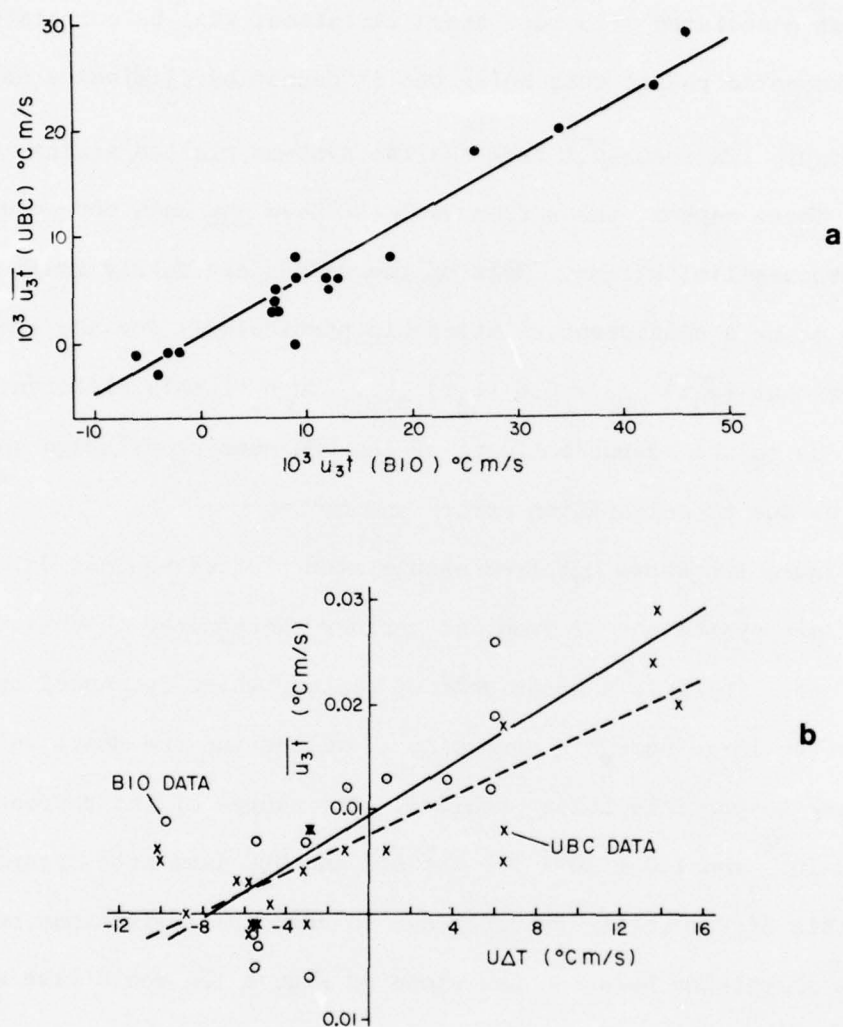


Figure 12. (a) Comparison of $\overline{u_3 t}$ from the BIO and UBC systems. The line has a slope of 0.6.
 (b) Heat flux $\overline{u_3 t}$ as a function of $U\Delta T$, with regression lines for BIO thermistor data (solid) and UBC data (dashed).

and the sensible heat flux is much smaller than the latent heat flux (when it was measured, and hence much of the time since the overall conditions were similar). Under such conditions the temperature signals may be contaminated by the response of saline films on the thermistors to moisture fluctuations (Friehe and Schmitt, 1976). This would give $\overline{u_3 t}$ values that are too large, and apparent cospectra that have relatively larger values at higher frequencies than do the $\overline{u_1 u_3}$ cospectra. Such effects could explain the positive intercepts in Fig. 12b and the scattered values.

4.5 Humidity

During a four-hour period, satisfactory recordings of Lyman-alpha, Brady and aluminum oxide humidity data were made (Runs 6 to 9, Tables 1 and 5). Unfortunately, there was an offset change for the Gill velocity values near the start of Run 6 and the quantities dependent on velocity cannot be used for this run as analyzed. Reasonable correlations of mean humidity between the three sensors were obtained, but the sensors had some calibration drifts and the UBC sensors had limited frequency response.

The sensors were separated 90 cm horizontally and 85 cm vertically. Sonic u_3 was used with the Lyman-alpha data while Gill u_3 was used with the Brady and aluminum oxide data to derive the moisture flux, $\overline{qu_3}$. The data in Table 5 are not corrected for response limitations.

The spectrum from the unshielded Lyman-alpha (ultraviolet) absorption humidimeter for Run 6 (Fig. 13a) resembles that of downwind velocity and shows an approximate $-5/3$ power law starting at 0.3 Hz. The two UBC humidity sensors showed much lower humidity fluctuation levels at all frequencies and also additional attenuation with frequencies from 0.02 Hz up. Of the two, the Brady type sensor had the higher spectral levels at 0.01 to 0.02 Hz, but its response fell off more rapidly at frequencies from 0.02 to 0.1 Hz.

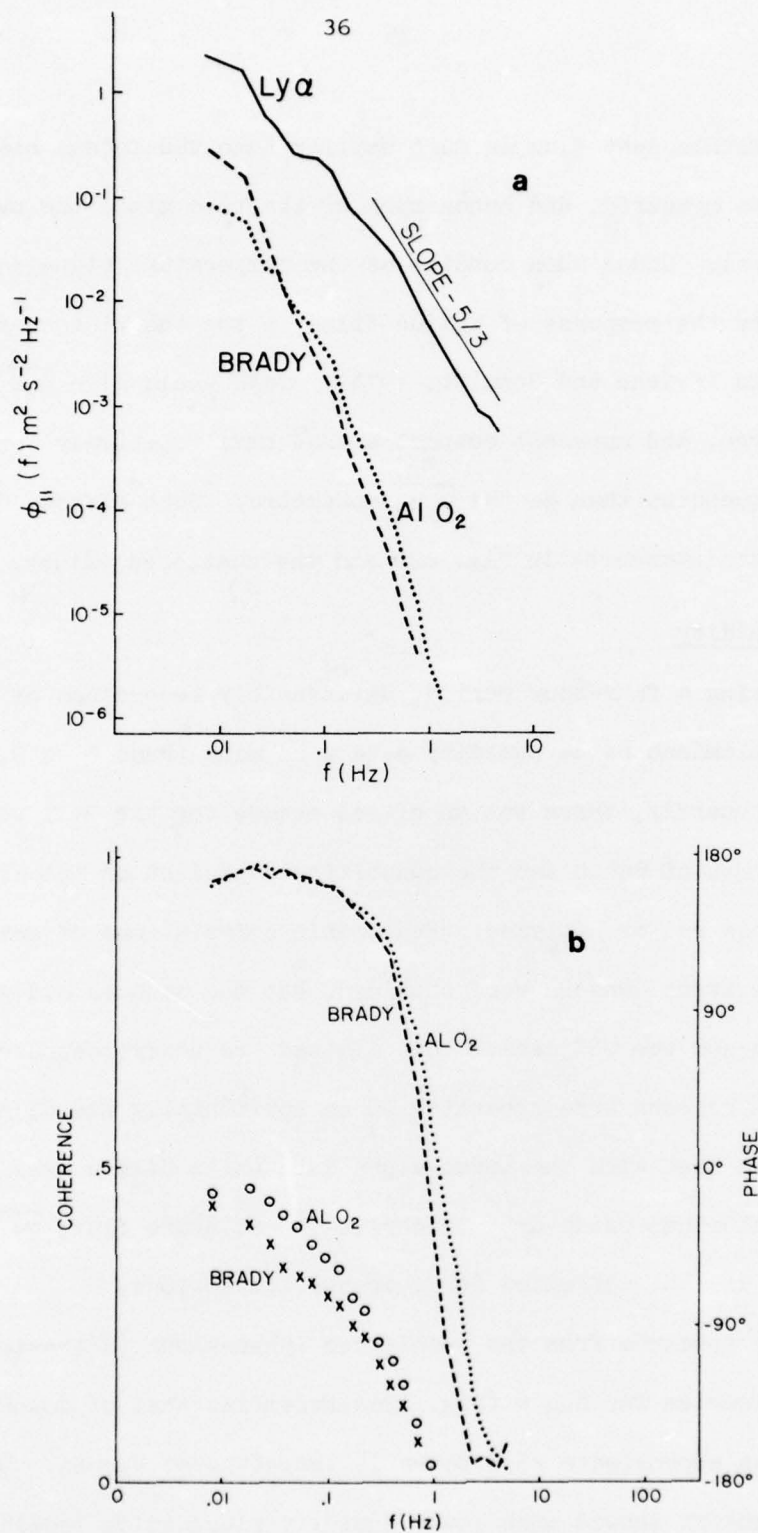


Figure 13. (a) Humidity spectra for Run 6; Lyman-alpha (solid); Brady (dashed), and AlO_2 sensor (dotted). (b) Coherence between Brady and Lyman-alpha (dashed line) and between AlO_2 and Lyman-alpha (dotted line). Phase, relative to Lyman-alpha, of Brady (X) and AlO_2 (O) humidity signals.

The coherence between the Lyman-alpha and the other sensors is good up to 0.17 Hz but a phase lag of 90° develops by 0.13 Hz in the Brady and 0.3 Hz in the aluminum oxide sensor (Fig. 13b). Very little of this phase shift can be accounted for by sensor separation. Thorpe (1973) found that there is a delay other than a simple R-C filter type smoothing of the fluctuations measured by a Brady relative humidity sensor and that this could not be accounted for by temperature effects in the sensor.

Neither of the UBC humidity sensors in their present form have adequate frequency response for eddy flux measurements of the type reported here. The aluminum oxide sensor had large calibration shifts because of salt contamination and will no longer be used. Hopefully, the Brady sensor frequency response can be improved or corrected for. Part of the frequency response loss may be due to the protective shield; the Brady sensor has been relocated to improve its flushing.

The low spectral values for the UBC sensors seem peculiar because visual examination of the original records shows that the three follow one another rather well for periods of a minute and longer. The phase difference of about 20° (Fig. 13b) for frequencies about 0.01 Hz would suggest that the error in amplitude would be moderate if an RC type of response is occurring. The UBC calibrations have been checked and while they have some uncertainty the large discrepancy cannot be accounted for by calibration errors; the BIO calibrations must be reasonable since the $\sigma_q / \Delta Q$ and C_q values are reasonable.

The Brady sensor is supposed to respond to relative humidity. In calculating σ_q and $\overline{u_3 q}$ values temperature effects have been ignored - i.e. the relative humidity values have been multiplied by the interpolated saturated values of Q based on the air temperatures observed with the

TABLE 5
HUMIDITY DATA

S = water surface; P = hand-held psychrometer at 9m;
L = Lyman-alpha; B = Brady; A = aluminum oxide

Run	Relative Humidity	Water Vapour Density \bar{Q} gm/m ³	Density ΔQ	$\sigma_q/\Delta Q$	\overline{qu}_3 gm/m ² s	$C_Q \times 10^3$ $\overline{qu}_3/\Delta QU_{10}$
6	S 100	12.1	-	-	-	-
	P 68.7	8.0	4.1	-	-	-
	L	7.8	4.4	0.088	0.050	1.51
	B 69.0	8.1	4.0	0.026	-	-
	A	7.5	4.6	0.018	-	-
7	S 100	12.1	-	-	-	-
	P 69.7	8.1	4.0	-	-	-
	L	8.1	4.0	0.097	0.049	1.66
	B 10.0	8.1	4.0	0.030	0.007	0.20
	A	7.6	4.5	0.010	0.006	0.16
8	S 100	12.1	-	-	-	-
	P 70.5	8.3	3.8	-	-	-
	L	8.3	3.8	0.091	0.047	1.47
	B 70.4	8.3	3.8	0.025	0.004	0.12
	A	7.9	4.2	0.027	0.006	0.15
9	S 100	11.9	-	-	-	-
	P 72.3	8.8	3.1	-	-	-
	L	8.7	3.2	0.078	0.026	1.05
	B 70.4	8.6	3.3	0.022	0.002	0.08
	A	8.5	3.4	0.051	0.003	0.11

$$C_q = (1.42 \pm 0.26) \times 10^{-3}$$

mercury thermometers of the psychrometer. The temperature fluctuations also have an effect but under the observed conditions this effect is only about 10%. With temperature fluctuations generally in phase as is the case for these runs and well correlated (as is usually the case) the corrected σ_q and $\overline{u_3 q}$ values would be 10% larger and the spectral values 20% larger, not nearly enough to account for the observed discrepancies.

Both the Brady and AlO_2 sensors have some hysteresis. Perhaps the hysteresis is the cause of the low-frequency attenuation in amplitude with small phase shift. The higher frequency RC-type rolloff is due to limited response of the sensor.

Water surface temperatures were measured with a bucket thermometer and the saturated air in contact with the water is assumed to have been at the same temperature. The average value of the evaporation coefficient, $C_Q = (1.42 \pm 0.26) \times 10^{-3}$ for the Lyman-alpha and sonic u_3 data, agrees well with existing observations (e.g., Pond *et al.*, 1971; Smith, 1974; Friehe and Schmitt, 1976).

5. SUMMARY

The experiment achieved its main objective: to demonstrate that the BIO system and the IOUBC system would run well together and measure essentially the same quantities. The agreement for velocity measurements was good if corrections were applied to account for the response limitation of the Gill anemometer and for an apparent calibration difference between the sonic and Gill anemometers. The thrust anemometer results were more scattered because of noisy operation, but nevertheless also agreed with the sonic and Gill anemometer results fairly well. The overall results were consistent with similar measurements obtained at other sites. Temperature measurements with the two systems showed general agreement for temperature fluctuation and fluxes, but not for mean values. There were problems with

calibration, drift, frequency response, and noise of the temperature sensors which we shall try to reduce in future experiments. The limited humidity measurements showed that there is reasonable coherence between sensors at low frequencies but that the IOUBC sensors have reduced response at moderate frequencies as well as a time constant effect at higher frequencies.

As a result of this trial, development of a Mark 8 thrust anemometer has been undertaken for measurements at a stable platform near Halifax. It will use proximity transducers instead of differential transformers, and requires a less elaborate set of springs. A counterbalanced design for the horizontal components and much higher resonant frequency (> 60 Hz) should substantially reduce the vibration problems reported here for the Mark 6 and 7 anemometers. A thermistor will be mounted in an air passage in the case of the anemometer with its socket inverted so that moisture will drain out instead of in.

The need for a fast-response humidity sensor which can survive in a marine climate remains unfulfilled. The Lyman-alpha sensor performs well when carefully handled but has large power consumption and calibration drift. The Brady sensor needs improved frequency response and calibration stability.

6. ACKNOWLEDGEMENTS

The Mark 7 thrust anemometer was designed and built by P.F. Kingston and D.F. Knox.

The development of the IOUBC system and its deployment in this experiment were supported by the U.S. Office of Naval Research (Contract N00014-66-C-0047 under Project 083-207) and the National Research Council of Canada (Grant A 8301)

We are also very grateful to the Atmospheric Environment Service, DOE, for allowing us to use their facilities on Sable Island, and to the personnel of the weather station for their help.

7. REFERENCES

- DOBSON, F.W., R.F. BROWN, and D.R. CHANG. A set of programs for analysis of the time series data including fast Fourier transform spectral analysis. BIO Report BI-C-74-2, 334 pp.
- FRIEHE, C.A. and K.P. SCHMITT. 1976. Parameterization of air-sea interface fluxes of sensible heat and moisture by bulk aerodynamic formulas *J. Phys. Oceanogr.*, 6, 801-809.
- JAPAN-U.S. JOINT STUDY GROUP. 1971. Development of sonic anemometer-thermometer and its application to the study of the atmospheric surface layer. WDD Technical Note 6, Disaster Prevention Research Institute, Kyoto University, Japan, 250 pp.
- POND, S., G.T. PHELPS, J.E. PAQUIN, G. McBEAN and R.W. STEWART. 1971. Measurements of the turbulent fluxes of momentum, moisture and sensible heat over the ocean. *J. Atmos. Sci.*, 28: 901-917.
- POND, S. AND W. LARGE. 1976. A system for remote measurements of air sea fluxes at moderate to high wind speeds (in preparation).
- SMITH, S.D. 1969. A sensor system for wind stress measurement. BIO Report BI-1969-4, 64 pp.
- SMITH, S.D. 1974. Program A to D for analogue-to-digital conversion and processing of time series data. BIO Report BI-C-74-1, 68 pp.
- SMITH, S.D. and E.G. BANKE. 1975. Variation of the sea surface coefficient with wind speed. *Quart. J. Roy. Met. Soc.*, 101: 665-673.
- THORPE, M.R. 1973. The frequency response of a micro-thermistor and a Thunder Scientific humidity sensor in atmospheric turbulence. BIO Report BI-R-73-2, 12 pp.